Difference in "Base Pair to Termini" Affects the Enzymatic Digestion of Nanoparticle-Bonded DNA

Wei Ling Tan, Weijie Qin, and Lin Yue Lanry Yung*

Department of Chemical and Biomolecular Engineering, National University of Singapore, 10 Kent Ridge Crescent, Singapore 119260, Singapore

Received September 21, 2006

Revised Manuscript Received November 14, 2006

Self-assembly of metallic nanoparticles to form one-, two-, and three-dimensional functionalized structures is of immersed interest recently due to their potential applications in various fields such as the biosensor, diagnostics, nanocircuitry, catalysis, high-density data storage, magnetic recording, bioseparation, nanostructure construction, and biomimetics.[1−5] Among the self-assemblies of metallic nanoparticles, gold nanoparticles (nAu) conjugated with single-stranded DNA (ssDNA) is most ubiquitous because of the complementary recognizability and programmability of DNA. Kiehl and co-workers have demonstrated the first use of self-assembled two-dimensional DNA lattices to organize 6 nm nAu thiolated with ssDNA into periodic striped patterns with an interparticle spacing ranging from 15 to 25 nm.[6] The DNA lattice is built from a two-tile system where one tile is modified with a ssDNA for positioning the complementary ssDNA-modified nAu through hybridization. More accurate control of interparticle spacing was achieved by Zhang and co-workers where DNA tiles with cross structure composed of four arm DNA branch junctions form the scaffold that allows 5 nm nAu to evenly space out.[7] Using a similar strategy, Zheng and co-workers have shown that, by using triangular double crossover molecules as tiles, highly ordered arrangement of different sizes nAu in a two-dimensional array can be achieved.[8] The advantage of DNA-mediated self-assembly is the high specificity assured. In addition, the inherent flexibility in altering the length of ssDNA to control the dimension of nAu−ssDNA conjugates and eventually that of the nanostructure make it the biological linker of choice.[9]

The conjugation of ssDNA to nAu is like a surface reaction, and there is no control on the exact number of ssDNA conjugating onto a single nAu. This inability to control the number of ssDNA thiolated onto nAu can be overcome by agarose gel electrophoresis, where nAu bonded with different numbers of ssDNA can be separated by mass.[10,11] For nAu bonded with ssDNA of 50 bases or less in length, however, this method is inadequate because the electrophoretic mobility difference between conjugates having different number of ssDNA is too low for effective separation. To overcome this, we have previously shown that, after gel electrophoresis, nAu bearing a specific number of double-stranded DNA (dsDNA) longer than 50 base pairs (bp) can be cleaved through restriction endonuclease to yield the nanoparticle with a specific number of short ssDNA strands (<20 bp).[9] In addition, dsDNA can be sequenced such that there are recognition sites of various type II restriction endonucleases along the strand, and hence the length can be altered by using different enzymes at their respective recognition sites.

* Corresponding author. E-mail: cheyly@nus.edu.sg.

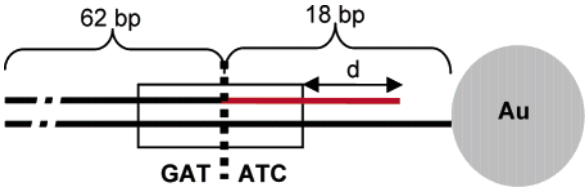

Figure 1. dsDNA bonded on 10 nm nAu via thiol linkage. The strand bonded to nAu is 80-base long. The other strand varies from 67- to 70-base. Cutting side of *Eco*RV is at the middle of the GATATC sequence.

Restriction endonuclease can only cleave at the internal part, and not the end, of a dsDNA strand. The product obtained afterward is normally also in double-stranded form (see Figure 1). If the length of product from the digestion of dsDNA bonded to nAu, or base pair to termini, *d*, is short enough, dehybridization occurs readily at room temperature and thus yields the nAu−ssDNA for various applications that require the Watson−Crick base pair matching. In this study, we demonstrated the effect of varying *d* on digestion efficiency and determined the shortest *d* (minimum number of bp to termini) needed for efficient enzymatic digestion of dsDNA bonded to 10 nm nAu.

10 nm nAu used in conjugation was prepared using the typical controlled reduction of hydrogen tetrachloroaurate(III) hydrate ($HAuCl_4$) solution by trisodium citrate and tannic acid. DNA oligonucleotides with and without 5′ thiol linker modification (Figure 2) were purchased from Integrated DNA Technologies. Annealing of the complementary oligonucleotides to form dsDNA was conducted in 75 mM NaCl and 50 mM Tris buffer at 95 °C with a gradual cooling after the initial heating. Totally four different dsDNAs were used in this study, and they each vary by a base as shown in Figure 2. Conjugation of dsDNA was done with the stoichiometric ratio of 3 dsDNA:1 nAu in a buffer system of 100 mM Tris and 0.05 mM NaCl. Each nAu−dsDNA conjugate in this study bears only one of the four types of dsDNA sequences. dT_5 was then added to passivate the nAu surface before the enzymatic digestion. *Eco*RV is the type II restriction endonuclease used in this study. It recognizes and cleaves the sequence GATATC specifically. As shown in Scheme 1, after *Eco*RV digestion, the samples were centrifuged at 13 500*g*. Afterward, the supernatant that contains digested dsDNA fragments was collected. Undigested strands bonded on nAu were released by excess dithiothreitol (DTT) through thiol exchange reaction. Digested dsDNA and undigested strands were then pooled together for 12% polyacrylamide gel electrophoresis (PAGE) followed by ethidium bromide staining for digestion efficiency analysis. Alternatively, ethylenediaminetetraacetic acid (EDTA) was added immediately after digestion to inhibit *Eco*RV. After centrifugation, the supernatant was collected for PAGE. More detailed protocols are shown in the Supporting Information. It should be noted in Scheme 1 that the dehybridized fragments in the supernatant after *Eco*RV digestion are the short fragments (red fragment shown in Figure 1) dissociated from double helix formation due to its short length.[9]

The *Eco*RV digestion results of nAu−dsDNA conjugates are shown in Figure 3. Lanes 3 and 6 in (A) and lanes 3 and 6 in (B) show the undigested conjugates (negative control) with $d = 5$, 4, 3, and 2, respectively. As compared to the standard DNA ladder, all undigested bands correspond to 80 bp in length,

10.1021/bm060904y CCC: $37.00
Published on Web 01/19/2007

dsDNA

```
5′-GCAGTAACGCTATATTGCCGAGAAGGTTTGGATTTGCTGGGTACAACTAGGCTTCAC
3′-CGTCATTGCGATATAACGGCTCTTCCAAACCTAAACGACCCATGTTGATCCGAAGTG

AGGATATCX-3′
TCCTATAGAGTGATAACGCGTTC-SH 5′
```

dT_5

```
3′-TTTTT-C6-SH-5′
```

Figure 2. DNA sequences used. Totally 4 dsDNA used in the study with $d = 2-5$. For $d = 5$, X = TCACT; $d = 4$, X = TCAC; $d = 3$, X = TCA; $d = 2$, X = TC. dT_5 used for surface passivation of nAu.

Scheme 1

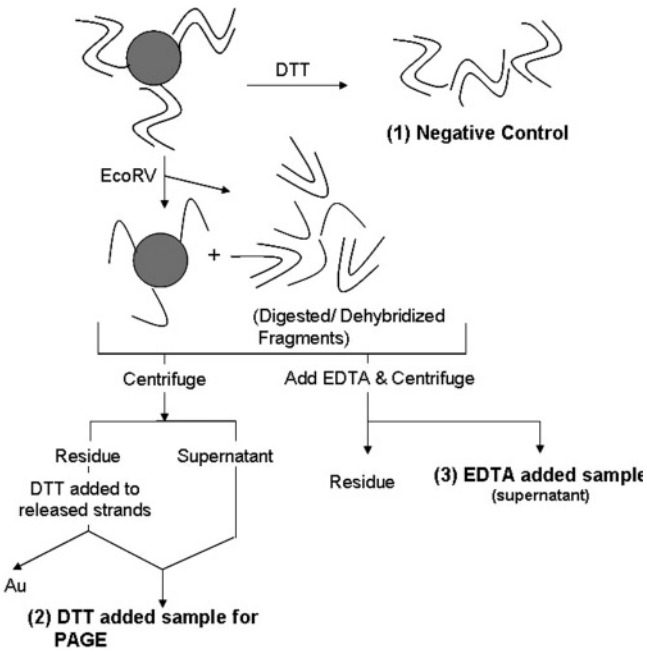

indicating that dsDNA bonded to nAu is intact and stable. Lanes 1 and 4 in (A) and lanes 1 and 4 in (B) show the digested dsDNA fragments with $d = 5$, 4, 3, and 2, respectively. All digested bands correspond to 62 bp in length, indicating that the specificity of *Eco*RV digestion and the presence of nAu do not affect the sequence recognition. The vague bands at 80 bp correspond to the undigested dsDNA. Based on the fluorescent quantification in Table 1, 100% digestion efficiency is achieved when $d = 5$. For $d = 3$ and 4, the efficiencies are slightly lower (approximately 90%). When $d = 2$, the digestion efficiency decreases substantially and is below 80%. The undigested fragments of $d = 4$ and 3 dsDNA are present in the gel, although the bands are not very visible to naked eyes.

The addition of EDTA at the end of the reaction period was to inhibit the *Eco*RV digestion by chelating away Mg^{2+} ion in the reaction mixture. Lanes 2 and 5 in both (A) and (B) of Figure 3 show the digested dsDNA fragments with $d = 5$, 4, 3, and 2, respectively, with EDTA inhibition. No band at 80 bp region was found because undigested dsDNA residue was not released from nAu under the EDTA treatment. Based on the 62 bp band intensity, the difference between DTT and EDTA treatments is negligible, implying that the time lag due to centrifugation before the addition of excess DTT does not give rise to further digestion of dsDNA bound on nAu. This also indicates that excessive DTT is effective in stopping the *Eco*RV activity. It should be noted that the usage of EDTA broadens the band, which leads to higher background noise in fluorescence quantification. Hence, the DTT treatment was used for digestion efficiency determination shown in Table 1.

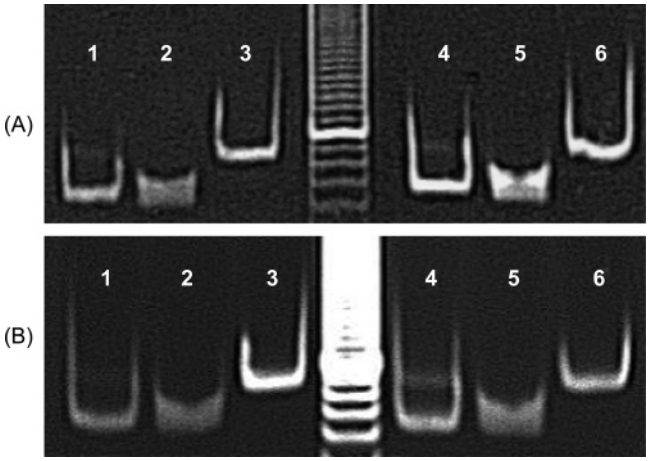

Figure 3. Digestion of nanoparticle−DNA conjugates with different d by *Eco*RV. (A) Excluding the 10 bp ladder, lanes 1−3 correspond to digested conjugate ($d = 5$) with (1) excess DTT added, (2) EDTA added, and (3) negative control. Band detected at 62 bp for (1) and (2), band detected at 80 bp for (3). Lanes 4−6 correspond to digested conjugate ($d = 4$) with (4) excess DTT added, (5) EDTA added, and (6) negative control. Band detected at 62 bp for (4) and (5), band detected at 80 bp for (6). (B) Lanes 1−3 correspond to digested conjugate ($d = 3$) with (1) excess DTT added, (2) EDTA added, and (3) negative control. Band detected at 62 bp for (1) and (2), band detected at 80 bp for (3). Lanes 4−6 correspond to digested conjugate ($d = 2$) with (4) excess DTT added, (5) EDTA added, and (6) negative control. Bands detected at both 62 bp and 80 bp for (4), band detected at 62 bp for (5), band detected at 80 bp for (6).

Table 1. Digestion Efficiency of Conjugated and Free dsDNA with Different Lengths of d

	digestion efficiency			
	nAu−dsDNA conjugate		free DNA	
d	average	st. dev.	average	st. dev.
5	100.0		100.0	
4	88.2	2.5	95.7	4.3
3	90.5	1.8	81.0	4.5
2	78.8	3.2	75.2	2.3

The electrophoresis of digested free DNA (see Supporting Information) shows a similar trend that digestion efficiencies decrease with decreasing d. The quantification results in Table 1 show the digestion efficiencies drop from 100% to 75.2% as d decreases from 5 to 2. This trend is consistent with the conjugate digestion case. It is believed that with more base pairs next to the recognition and cutting site, the enzyme can position the substrate dsDNA better, resulting in higher digestion efficiency. In addition, the similarity in efficiencies between conjugated and free DNA digestion shows that the presence of nAu does not inhibit or affect the enzyme binding to dsDNA and the subsequent digestion. For both cases, complete digestion was only found when d is 5. Hence, for the preparation of nAu bearing a specific number of short ssDNA (<20b) for nano-

structure construction, it is recommended that dsDNA with $d = 5$ or more be used as the starting material. It should be noted that d might be sequence or restriction endonuclease sensitive. Therefore, it should not be taken that this figure is capable of universal application. For enzymes with lower digestion efficiency, a longer d may be required. We have also observed from unpublished data that the efficiencies of conjugate digestion may vary slightly with different batches of enzymes even though the overall trend is maintained to be the same.

The challenge of maintaining high digestion efficiency for nAu-bonded dsDNA to produce desired nAu−ssDNA building blocks includes the strict control on the number of dsDNA on the nAu surface to prevent formation of uncontrolled network structure, as well as the retention of dsDNA double-helix conformation and its availability for enzymatic digestion. While control over the number of dsDNA bonded to each nanoparticle can be done using aforementioned means, retention of conjugated dsDNA double-helix conformation was done by passivating the nAu surface with dT_5 as shown in Figure 2. By passivating the surface of nAu, the wrapping of dsDNA onto the surface of nAu through nonspecific interactions can be prevented. This is especially vital when the dsDNA are guanine (G) and cytosine (C) rich because their affinity for the surface binding is higher.[10] We have previously shown that the lack or inadequate surface passivation can cause a reduction in digestion efficiency.[12] This decrease in efficiency may be attributed to the adsorption of enzymes onto the nanoparticle surface or the nonspecific binding of dsDNA on nAu. Mixing dsDNA with cationic conducting polymers, however, seems to have a minimal effect on the double-helix structure.[13] Besides conferring protections to the conformation of the adsorbed dsDNA, surface saturation also reduces nAu aggregation in aqueous medium especially at high electrolyte concentration where the stability of the nanoparticles is usually compromised. The usage of proteins to saturate nanoparticle surface through nonspecific interactions has been proposed by several other research groups. This includes the use of lysozyme,[14,15] bovine serum albumin (BSA),[15,16] or IgG[17] on silica nanoparticles and cytochrome *c* on colloidal gold.[17] The usage of BSA had been considered in this study, but surface saturation with dT_5 was opted because the physisorbed protein may fall off the nanoparticle surface during the processing of conjugates, such as centrifugation, and result in nanoparticle aggregation.

In conclusion, we have shown that the digestion of nAu-conjugated DNA is similar to respective free DNA digestion. The digestion efficiencies decrease with shorter base pairs to termini, with $d = 5$ being the minimum base pairs to termini required to provide efficient *Eco*RV digestion.

Acknowledgment. We appreciate the financial support from the National University of Singapore, faculty research program PS030157.

Supporting Information Available. Experimental procedures and gel image of free DNA digestion. This material is available free of charge via the Internet at http://pubs.acs.org.

References and Notes

(1) Cheng, G. J.; Romero, D.; Fraser, G. T.; Walker, A. R. H. *Langmuir* **2005**, *21*, 12055−12059.
(2) Mirkin, C. A. *Inorg. Chem.* **2000**, *39*, 2258−2266.
(3) Parak, W. J.; Gerion, D.; Pellegrino, T.; Zanchet, D.; Micheel, C.; Williams, S. C.; Boudreau, R.; Le Gros, M. A.; Larabell, C. A.; Alivisatos, A. P. *Nanotechnology* **2003**, *14*, R15−R27.
(4) Chitu, L.; Chushkin, Y.; Luby, S.; Majkova, E.; Satka, A.; Ivan, J.; Smrcok, L.; Buchal, A.; Giersig, M.; Hilgendorff, M. *Mater. Sci. Eng., C* **2007**, *27*, 23−28.
(5) Hou, Y. L.; Kondoh, H.; Ohta, T. *Chem. Mater.* **2005**, *17*, 3994−3996.
(6) Le, J. D.; Pinto, Y.; Seeman, N. C.; Musier-Forsyth, K.; Taton, T. A.; Kiehl, R. A. *Nano Lett.* **2004**, *4*, 2343−2347.
(7) Zhang, J. P.; Liu, Y.; Ke, Y. G.; Yan, H. *Nano Lett.* **2006**, *6*, 248−251.
(8) Zheng, J. W.; Constantinou, P. E.; Micheel, C.; Alivisatos, A. P.; Kiehl, R. A.; Seeman, N. C. *Nano Lett.* **2006**, *6*, 1502−1504.
(9) Qin, W. J.; Yung, L. Y. L. *Langmuir* **2005**, *21*, 11330−11334.
(10) Parak, W. J.; Pellegrino, T.; Micheel, C. M.; Gerion, D.; Williams, S. C.; Alivisatos, A. P. *Nano Lett.* **2003**, *3*, 33−36.
(11) Zanchet, D.; Micheel, C. M.; Parak, W. J.; Gerion, D.; Alivisatos, A. P. *Nano Lett.* **2001**, *1*, 32−35.
(12) Qin, W. J.; Yung, L. Y. L. *Biomacromolecules* **2006**, *7*, 3047−3051.
(13) Dawn, A.; Nandi, A. K. *Langmuir* **2006**, *22*, 3273−3279.
(14) Vertegel, A. A.; Siegel, R. W.; Dordick, J. S. *Langmuir* **2004**, *20*, 6800−6807.
(15) Norde, W.; Favier, J. P. *Colloids Surf.* **1992**, *64*, 87−93.
(16) Norde, W.; Anusiem, A. C. I. *Colloids Surf.* **1992**, *66*, 73−80.
(17) Buijs, J.; Norde, W.; Lichtenbelt, J. W. T. *Langmuir* **1996**, *12*, 1605−1613.

BM060904Y